Supporting Information

Ultra-high Thermally Conductive and Rapid Heat Responsive Poly(benzobisoxazole) Nanocomposites with Self-aligned Graphene

Weifeng Zhao[1,2], Jie Kong[1]*, Hu Liu,[3] Qiang Zhuang[1], Junwei Gu[1] and Zhanhu Guo[3]*

[1]MOE Key Laboratory of Space Applied Physics and Chemistry, Shaanxi Key Laboratory of Macromolecular Science and Technology, School of Science, Northwestern Polytechnical University, Xi'an, 710072, P. R. China

[2]School of Materials and Chemical Engineering, Xi'an Technological University, Xi'an 710021, P. R. China

[3]Integrated Composites Laboratory (ICL), Department of Chemical & Biomolecular Engineering, University of Tennessee, Knoxville, TN 37996 USA

*Corresponding Authors: E-mail Address: kongjie@nwpu.edu.cn (J. K.);

zguo10@utk.edu (Z.G.)

Synthesis and Characterization of PBO Precursor (TBS-prePBO)

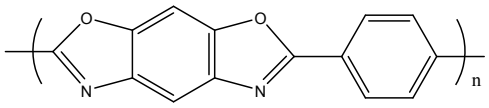

Figure S1 Chemical structure of PBO.

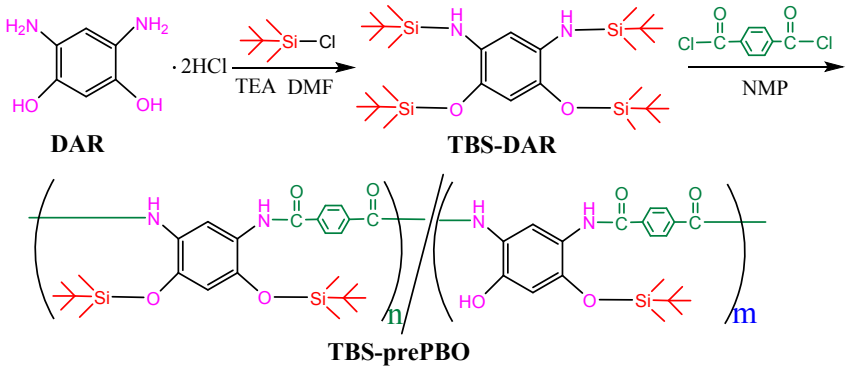

Figure S2 Synthesis of soluble PBO precursor (TBS-prePBO) via reaction of *tert*-butyldimethylsilyl group-functionalized 4, 6-diaminoresoisinol (TBS-DAR) and terephthaloyl chlorid.

As illustrated in **Figures S1-2**, the 4, 6-diaminoresorcinol dihydrochloride (DAR) is the main monomer for the synthesis of PBO. However, it has poor solubility in common solvents and is easily oxidized in air atmosphere, leading to the difficulty in the design and synthesis of the PBO precursor. To overcome this defect, *tert*-butyldimethylsilyl (TBS) was chosen as the functional unit of DAR to improve its solubility and stability.

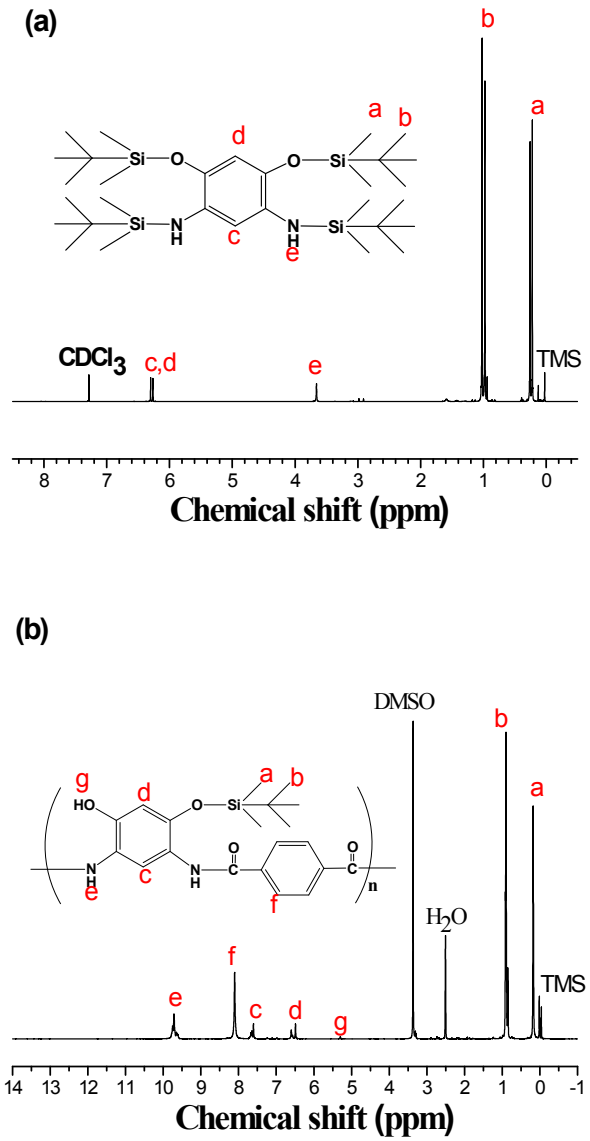

Figure S3 ^{1}H NMR spectrum of (a)TBS-DAR and (b)TBS-prePBO.

As shown in **Figure S3a**, the strong signals ascribed to the protons of TBS groups (H_a at 0.22–0.24 ppm, H_b at 0.97–1.02 ppm) are observed from the ^{1}H NMR spectrum of the prepared TBS-functionalized DAR (TBS-DAR). Especially, the $H_{a,b}$ in the TBS group and the $H_{c,d}$ (6.27-6.30 ppm) in the aromatic groups were determined to be TBS:

aromatic=60.3:2, which gave an evidence that all the hydroxyl and amine groups of DAR have been fully protected by the TBS groups.

As shown in **Figure S3b**, two resonance peaks attributed to the proton H_f of terephthaloyl chloride and the proton H_e of the secondary amine N-H (-C=O) were observed, which clearly suggested the progress of polycondension reaction. Moreover, compared with **Figure S3a**, the resonance peaks of H_c and H_e moved to a much higher chemical shift due to the presence of terephthaloyl groups, providing an obvious evidence for the condensation reaction. The integration ratio of methyl and aromatic protons was $(H_a+H_b):(H_c+H_d+H_f)$, i.e. 22.3:6, which was in correspondence with the TBS content around 75% in molar ratio on the main chain. It is lower than the expected value 30:6 for the TBS-prePBO with hydroxyl groups fully protected. It suggests that a partial weakening of the TBS has occurred during the polymerization process. As a result, the proton in the phenolic hydroxyl group (H_g, 5.29 ppm) was also detected as shown in **Figure S3b**.

The good solubility of TBS-DAR greatly facilitates the synthesis of PBO precursors by a benign condensation polymerization of TBS-DAR with terephthaloyl chloride in *N*-methyl-2-pyrrolidone solution. During the synthesis, an increase of the solution's viscosity is observed, giving a direct indication that there is a dramatic increase in the molecular weight as expected according to the general mechanism of the condensation polymerization. After precipitation in methanol and purification with water, a yellowish powder was obtained with a yield of 85%. The intrinsic viscosity of the obtained TBS-prePBO polymer was 0.36 dL g^{-1} in DMF at 30 °C.

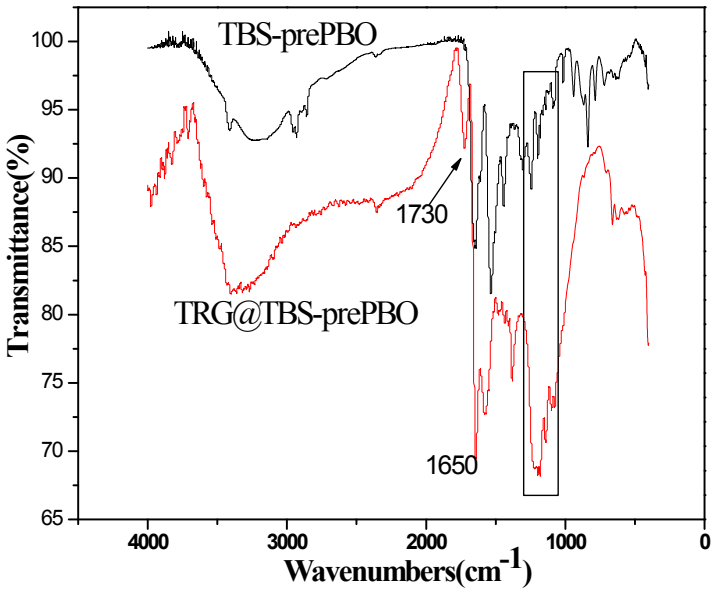

Figure S4 FT-IR spectrum of TBS-prePBO and the extracted TRG@TBS-prePBO hybrid.

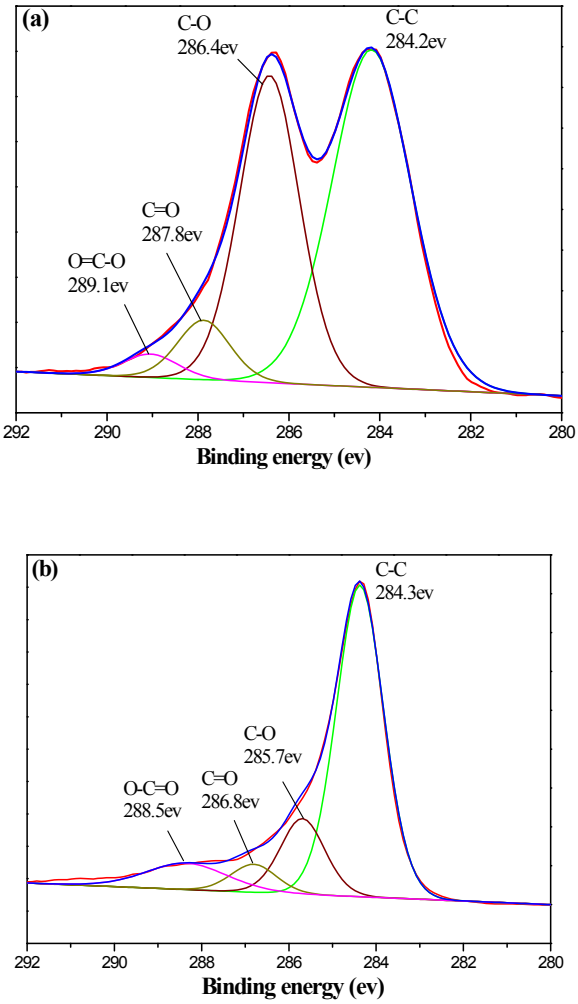

Figure S5 XPS spectra of (a) GO and (b) TRG reduced at 350 °C.

Table S1 List of the atomic composition of GO and TRG reduced at 350 °C measured by XPS.

Sample	C(atomic%)	O(atomic%)	N(atomic%)	S(atomic%)	Si(atomic%)	C/O ratio
GO	65.2	30.4	1.8	1.4	1.2	2.14
TRG@350°C	76.8	16.5	2.8	2.6	1.3	4.65

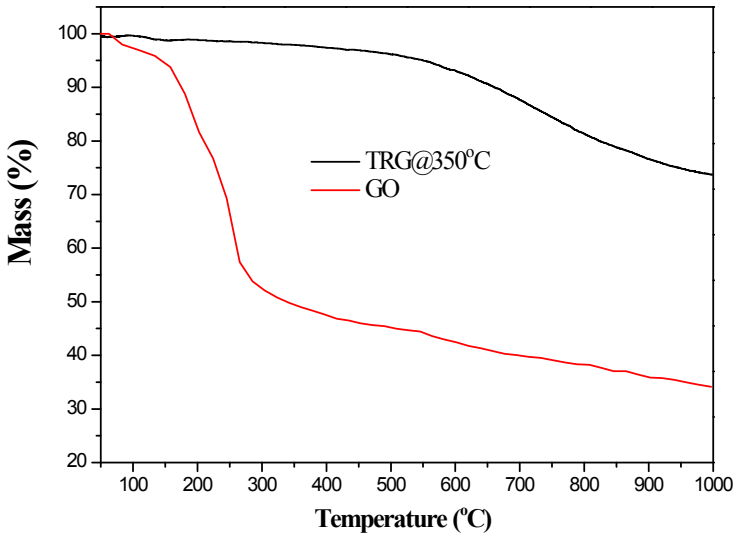

Figure S6 TGA curves of GO and TRG heated at 350 °C

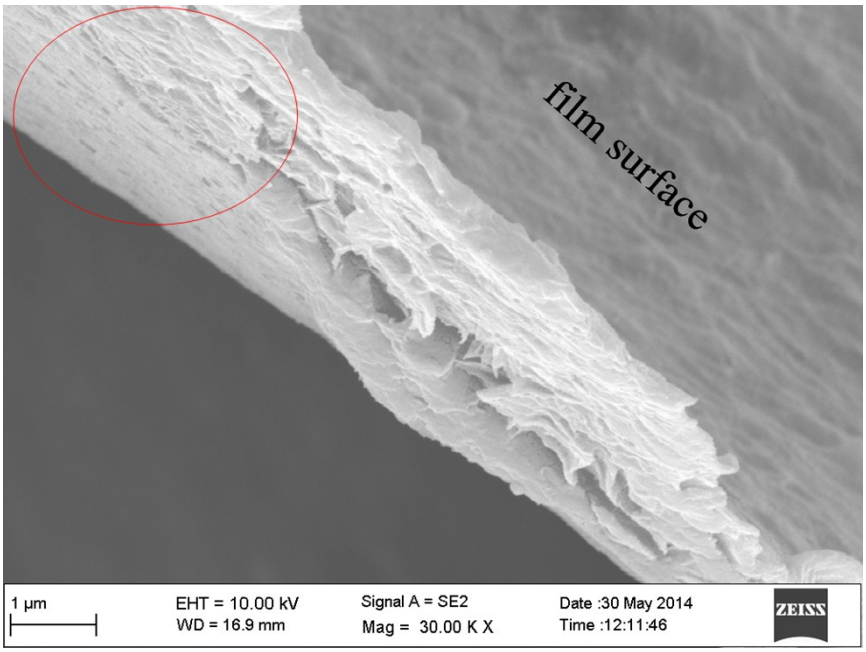

Figure S7 SEM images of the fracture surface of TRG/PBO nanocomposite film, the red cycle indicate a well-ordered parallel stacking of graphene sheets with their sheet plane parallel to the composite film surface

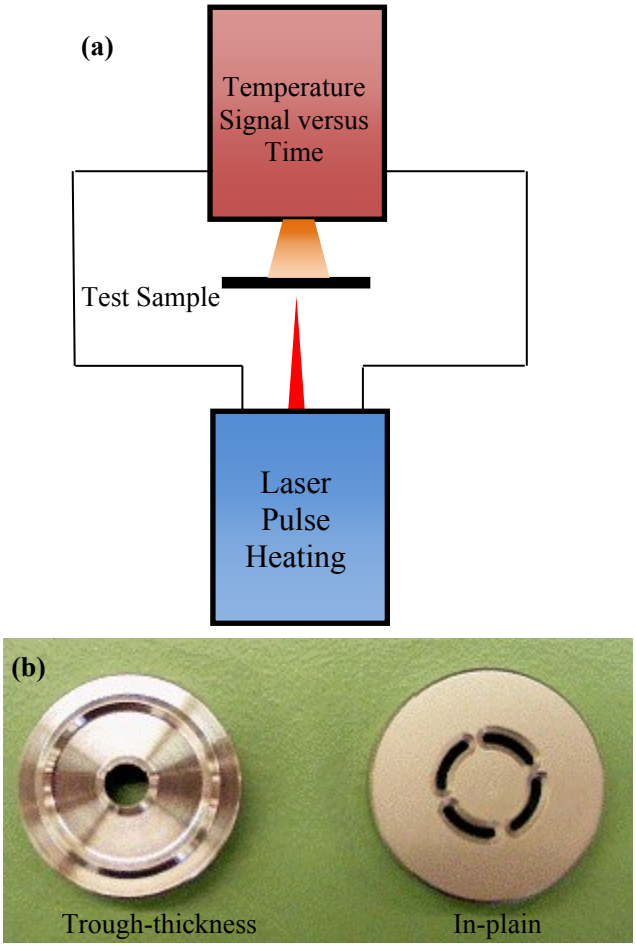

Figure S8 (a) Principle of operation of laser flash apparatus; and (b) sample carriers used for the through-thickness and in-plain thermal diffusivity test.

In the laser flash test, the samples were coated with graphite aerosol and then placed on a carrier as shown in Figure S8(b). In carrying out a measurement, the lower surface of the sample (Figure S8(a)) is irradiated by a short energy pulse. The pulse energy is absorbed and converted into a confined heat source on the lower surface. The heat waves diffuse through the sample and lead to a temperature rise on the upper surface of the sample. An infrared detector is directed to the upper surface and generates a highly sensitive signal on a response to the temperature change of the sample. The obtained

typical course of the normalized signals versus time is presented in Figure5 (A). Using the half time ($t_{1/2}$, time value at half signal height) and sample thickness (δ), the thermal diffusivity (D) can be given by means of the Parker formula[S1].

$$D = \frac{1.37\delta^2}{\pi^2 t_{1/2}} = \frac{0.1388\delta^2}{t_{1/2}}$$

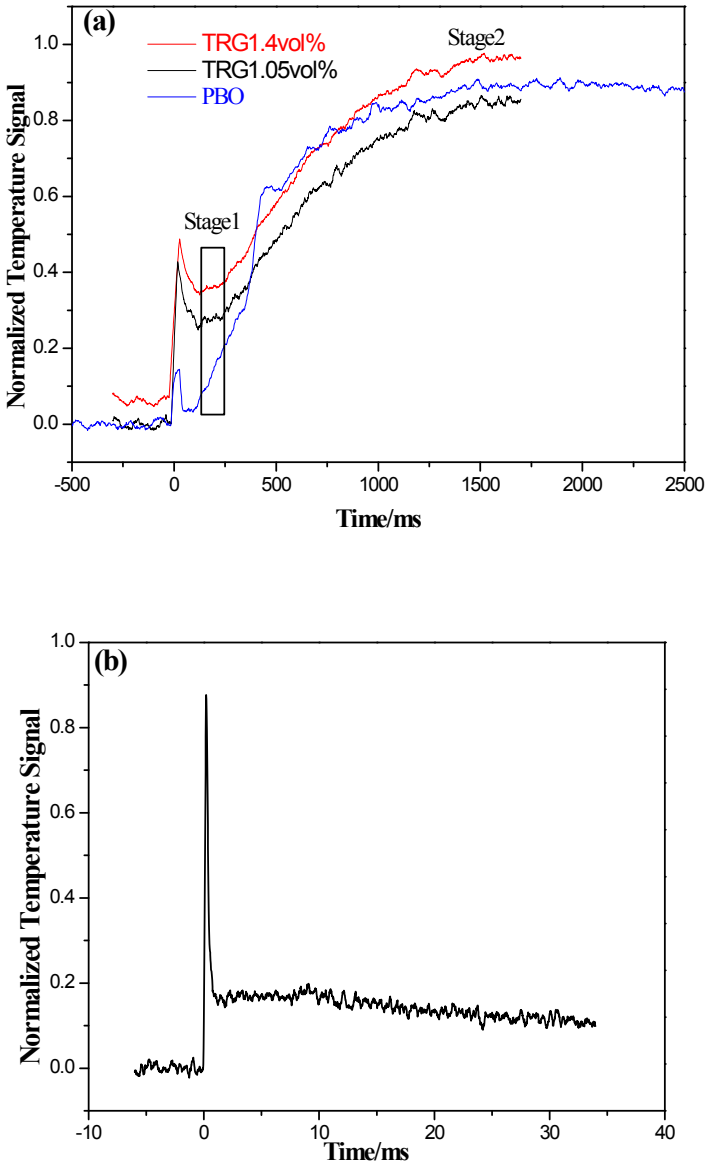

Figure S9 (a)In-plane direction temperature evolution of nanocomposite film surface at different time after pulsed laser heating; (b) the curve of temperature evolution typically measured for the stage1 incensement shown in (a) for the composite with 1.05vol% TRG loading

Table S2 Comparison of the thermal conductivity enhancement of polymer composites with various graphene-based materials.

Polymer matrix	Filler type	Filler fraction	Thermal conductivity (W/(m·K))	Method	Reference
PP	Graphene nanoplatelets	25 vol%	1.2	DSC	S2
PPS	Graphene nanoplatelets	40 wt%	4.4	Hot plate method	S3
LCP	Graphene nanoplatelets	30 wt%	2.5	ASTM E1225-04	S4
Epoxy	GO	20 wt%	5.8	Laser flash	S5
Epoxy	Graphene nanoplatelets	25 wt%	2.67	Hot plate method	S6
Epoxy	TRG	4 phr	1.9	Hot plate method	S7
Epoxy	Non-oxidized graphene	10 wt%	1.53	Laser flash	S8
Epoxy	Multilayer graphene	10 vol%	5.1	Laser flash	S9
Epoxy	Few layer graphene	25vol%	6.4	Laser flash	S10
Epoxy	Multilayer graphene	11.8wt%	33.5	ASTM D5470-06	S11
PBO	TRG	4.2vol%	50	Laser flash	This work

References:

[S1]WJ Parker, R J Jenkins, C P Butler and G L Abbott. J.Appl. Phys.,**1961**:1679

[S2] K Kalaitzidou , H Fukushima, L T Drzal. *Carbon,* 2007, 45, 1446–1452.

[S3] JW Gu, J. Du, J Dang, W.C Geng, SH Hu and QY Zhang. *RSC Adv*., 2014, 4, 22101

[S4] SN Leung, MO Khan, H Nagui and F. Dawson. *Appl. Phys. Lett.* 2014, 104, 081904

[S5] S Ganguli, A K Roy, D P Anderson , *Carbon* **2008**,46,806 .

[S6] WM Guo, GH Chen. *J. Appl. Polym. Sci.* 2014, 131, 40565

[S7] C C Teng , C C M Ma, C H Lu, SY Yang and et al. *Carbon,* 2011,49, 5107.

[S8] S H Song , K H Park , B H Kim and et al. *Adv. Mater*. 2013, 25, 732.

[S9] K M F Shahil, A A Balandin. *Nano Lett.* 2012, 12, 861.

[S10] A Yu , P Ramesh , M E. Itkis, E Bekyarova and R. C. Haddon. *J. Phys. Chem. C,* 2007, 111, 7565.

[S11] Q Li, Y F Guo, W Li, SQ Qiu and et al. *Chem. Mater.* 2014, 26, 4459.